Employment of methyl 2-pyridyl ketone oxime in manganese non-carboxylate chemistry: $Mn^{II}_2Mn^{IV}$ and $Mn^{II}_2Mn^{III}_6$ complexes†

Constantinos C. Stoumpos,[a] Theocharis C. Stamatatos,[b] Harikleia Sartzi,[a] Olivier Roubeau,[c] Anastasios J. Tasiopoulos,[d] Vassilios Nastopoulos,[a] Simon J. Teat,[e] George Christou*[b] and Spyros P. Perlepes*[a]

Received 8th August 2008, Accepted 28th October 2008
First published as an Advance Article on the web 9th January 2009
DOI: 10.1039/b813828a

The employment of the anion of methyl 2-pyridyl ketone oxime ($mpko^-$) as a tridentate chelating/bridging ligand in manganese chemistry is described. The inorganic anion (Br^-, ClO_4^-) used in the reaction affects the identity of the product. The reaction of $MnBr_2$ and one equivalent of mpkoH in the presence of a base affords $[Mn_3(OMe)_2(mpko)_4Br_2]$ (**3**), which is mixed-valence ($2Mn^{II}$, Mn^{IV}). The central Mn^{IV} atom in each of the two, crystallographically independent, centrosymmetric molecules is coordinated by four oximate oxygen atoms belonging to the $\eta^1{:}\eta^1{:}\eta^1{:}\mu$ $mpko^-$ ligands, and two $\eta^1{:}\mu$ MeO^- groups, while six coordination at each terminal Mn^{II} atom is completed by four nitrogen atoms belonging to the 'chelating' part of two $mpko^-$ ligands, and one Br^- ion. The Mn^{II} atoms have trigonal prismatic coordination geometry. The reaction of $Mn(ClO_4)_2{\cdot}6H_2O$, mpkoH and OH^- (1:2:1) in MeOH gives $[Mn_8O_4(OMe)(mpko)_9(mpkoH)](ClO_4)_4$ (**4**), which is also mixed-valence ($2Mn^{II}$, $6Mn^{III}$) and possesses the novel $[Mn_8(\mu_3\text{-}O)_4(\mu\text{-}OMe)(\mu\text{-}OR'')_2]^{11+}$ core. The latter possesses a U-shaped sequence of four fused $\{Mn^{II}Mn^{III}_2(\mu_3\text{-}O)\}^{6+}$ triangular units, with a Mn^{III}-Mn^{III} edge being shared between the central triangles. Variable-temperature, solid-state dc and ac magnetic susceptibility studies were carried out on complexes **3** and **4**. The dc susceptibility data for **3** in the 5.0–300 K range have been fit to a model with two J values, revealing weak ferromagnetic $Mn^{II}\cdots Mn^{IV}$ ($J = +3.4$ cm^{-1}) and $Mn^{II}\cdots Mn^{II}$ ($J' = +0.3$ cm^{-1}) exchange interactions. Fitting of the magnetization *vs.* H/T data by matrix diagonalization and including only axial anisotropy (ZFS, D) gave ground state spin (S) and D values of $S = 13/2$, $D = +0.17$ cm^{-1} for **3** and $S = 3$, $D = -0.09$ cm^{-1} for **4**. The combined work demonstrates the usefulness of $mpko^-$ in the preparation of interesting Mn clusters, without requiring the co-presence of carboxylate ligands.

Introduction

Molecular clusters of paramagnetic 3d metals at intermediate oxidation states continue to be a major research area of many groups around the world because of their fascinating physical properties, their occurrence in metal-containing biological sites, and the aesthetic beauty and complexity of their structures.[1] Manganese is a central player in the fields of bioinorganic chemistry and molecular magnetism. Manganese cluster chemistry has been receiving special attention for two main reasons: (i) the occurrence of this metal in a variety of redox enzymes,[2] the most important of which is the $\{CaMn_4\}$ water oxidizing complex (WOC) in the photosynthetic apparatus of green plants and cyanobacteria.[3] Bioinorganic chemists have been trying to recreate with synthetic models the structure, spectroscopic properties and/or function of this cluster unit;[4] (ii) high nuclearity Mn complexes often display large ground state spin (S) values[5] as a result of ferromagnetic exchange interactions and/or spin frustration effects.[6] If such molecules with large S values also possess significant magnetoanisotropy of the Ising (easy-axis) type, then they have the potential to be single-molecule magnets (SMMs).[7] These are individual molecules that possess a significant barrier (*vs.* kT) to magnetization relaxation and thus exhibit the ability to function as tiny magnets below their blocking temperature (T_B), representing a molecular, 'bottom-up' approach to nanomagnetism.[8]

Our group has had a strong interest over many years in the development of synthetic methods to manganese carboxylate and non-carboxylate clusters.[8,9] We have explored and successfully developed many new routes for the synthesis of polynuclear Mn complexes with nuclearities up to 84.[10] As part of this work, we have explored a wide variety of potentially chelating and simultaneously bridging organic ligands, including the anions of 2-(hydroxymethyl)pyridine and related ligands,[5b,5d,11] 2,6-pyridinedimethanol,[5b,5c,11b,12] 1,1,1-tris(hydroxymethyl)ethane,[13] triethanolamine,[14] *N*-methyldiethanolamine[14b,15] and the

[a]*Department of Chemistry, University of Patras, 265 04, Patras, Greece. E-mail: perlepes@patreas.upatras.gr; Tel: +30 2610 997146*
[b]*Department of Chemistry, University of Florida, Gainesville, Florida, 32611-7200, USA. E-mail: christou@chem.ufl.edu; Tel: +1 352 392 8314*
[c]*CNRS, UPR 8641, Centre de Recherche Paul Pascal (CRPP), Equipe "Materiaux Moléculaires Magnétiques", 115 avenue du Dr. Albert Schweitzer, Pessac, F-33600, France*
[d]*Department of Chemistry, University of Cyprus, 1678, Nicosia, Cyprus*
[e]*Advanced Light Source, Lawrence Berkeley National Laboratory, 1 Cyclotron Road, Mail Stop 2-400, Berkeley, CA 94720, USA*

† Electronic supplementary information (ESI) available: Plot of the out-of-phase ac susceptibility signals χ''_M *vs.* T for complexes **3** and **4** at 50, 250 and 1000 Hz. CCDC reference numbers 695721 and 69572. For ESI and crystallographic data in CIF or other electronic format see DOI: 10.1039/b813828a

 This journal is © The Royal Society of Chemistry 2009

gem-diol form of di-2-pyridylketone,[16] which have proven to foster formation of high nuclearity products. All these anions are alkoxide-based ligands (with or without pyridyl groups), and their alkoxide arm(s) often support ferromagnetic coupling between the metal ions that they bridge.[5b–d,11b–c,12b,17]

More recently, we and others have been investigating a number of other oxime-based ligands,[18] and one family of these have been the 2-pyridyl oximes and 2,6-pyridyl dioximes (Scheme 1), particularly methyl 2-pyridyl ketone oxime (mpkoH)[18,19] and 2,6-diacetylpyridine dioxime ($dapdoH_2$).[20] We recently reported, for example, the use of mpkoH in Mn *carboxylate* chemistry, which gave the $[Mn^{III}_3O(O_2CR')_3(mpko)_3]^+$ (**1**$^+$) cations in the presence of suitable counteranions. These were the initial examples of triangular Mn^{III} SMMs, formed by the reaction between compounds $[Mn^{III}_3O(O_2CR')_6(py)_3](ClO_4)$ (R′ = Me, Et, Ph; py = pyridine) and mpkoH;[19] in the absence of counteranions, the products are instead the clusters $[Mn^{II}_4Mn^{III}_4O_2(OH)_2(O_2CR')_{10}(mpko)_4]$ (**2**).[19e]

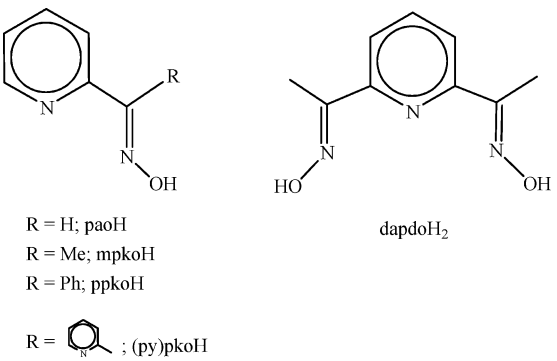

Scheme 1 Structural formulae and abbreviations of 2,6-diacetylpyridine dioxime and some 2-pyridyl oximes discussed in the text.

There is currently a renewed interest in the coordination chemistry of oximes, with the efforts of several research groups being driven by a number of considerations.[21] 2-pyridyl oximes[22,23] are a subclass of oximes whose anions are versatile ligands for a variety of research objectives (including μ_2 and μ_3 behaviour) and have been key ligands in several areas of molecular magnetism, including single-molecule[18] and single-chain[24] magnets. As an extension to the work with mpkoH, we have now asked what kind of products might result from the use of this ligand in Mn *non*-carboxylate chemistry. Since the carboxylate ($R'CO_2^-$) ions are structure-determining components in the cations **1**$^+$ and **2**, we anticipated that the absence of $R'CO_2^-$ from the reactions would give distinctly different products, and we have therefore explored this. In the present work, we have explored the reactions between mpkoH and Mn non-carboxylate starting materials under basic conditions. This has successfully led to $Mn^{II}_2Mn^{IV}$ and $Mn^{II}_2Mn^{III}_6$ clusters. The syntheses, structures and magnetochemical characterization of these compounds are described in this paper.

Experimental

Syntheses

All manipulations were performed under aerobic conditions using reagents and solvents as received. Methyl 2-pyridyl ketone oxime (mpkoH) was synthesized as described elsewhere.[25] *WARNING: Perchlorate salts are potentially explosive; such compounds should be synthesized and used in small quantities, and treated with utmost care at all times.*

$[Mn_3(OMe)_2(mpko)_4Br_2]$ (3). To a yellow solution of $MnBr_2$ (64 mg, 0.30 mmol) and mpkoH (41 mg, 0.30 mmol) in MeOH (20 mL) was added solid $LiOH·H_2O$ (13 mg, 0.31 mmol). The solid dissolved immediately followed by an abrupt colour change to dark brown. The solution was stirred for a further 15 min and then carefully layered with Et_2O (20 mL). After 2 days, small black crystals of **3**·0.5Et_2O were isolated by filtration, washed with Et_2O (3 × 3 mL) and dried in *vacuo.* Yield, 30%. The dried solid analyzed as solvent free **3**. Anal. Calc. for $C_{30}H_{34}Mn_3N_8O_6Br_2$: C, 38.85; H, 3.70; N, 12.09. Found: C, 38.82; H, 3.61; N, 12.13%. IR (KBr, cm^{-1}): 2922w, 2808w, 1596 s, 1552 m, 1474 s, 1436w, 1370 m, 1332w, 1254w, 1162w, 1138 m, 1096 m, 1066 s, 1046 s, 970w, 814w, 784 m, 746w, 710 s, 638 m, 554 s, 484w.

$[Mn_8O_4(OMe)(mpko)_9(mpkoH)](ClO_4)_4$ (4). To a stirred yellow solution of $Mn(ClO_4)_2·6H_2O$ (218 mg, 0.60 mmol) and mpkoH (163 mg, 1.20 mmol) in MeOH (20 mL) was added solid $LiOH·H_2O$ (25 mg, 0.60 mmol). The solid dissolved immediately followed by an abrupt colour change to dark brown. The stirring was discontinued and the solution allowed to slowly evaporate at room temperature. Polyhedral dark brown-black crystals of **4**·2MeOH formed over 2 days. The crystals were collected by filtration, washed with cold MeOH (5 × 5 mL) and dried in *vacuo.* Yield, ~60%. The dried solid analyzed as solvent free **4**. Anal. Calc. for $C_{71}H_{74}Mn_8N_{20}O_{31}Cl_4$: C, 37.32; H, 3.27; N, 12.26. Found: C, 36.90; H, 3.20; N, 11.86%. IR (KBr, cm^{-1}): 3438mbr, 2927w, 1598 m, 1556w, 1520w, 1476 m, 1436w, 1372w, 1334w, 1262w, 1158 m, 1146 m, 1092vsb, 1046 s, 971w, 828w, 778 m, 746w, 710 m, 692w, 660 m, 622 s, 587 m, 560 m, 494w, 462w.

Physical studies

Elemental analyses (C, H, N) were performed by the in-house facilities of the Chemistry Department, University of Florida. IR spectra (4000–450 cm^{-1}) were recorded using Perkin-Elmer 16 PC and Nicolet Nexus 670 FT-IR spectrometers with samples prepared as KBr pellets. Variable-temperature dc and ac magnetic susceptibility data were collected at the University of Florida using a Quantum Design MPMS-XL SQUID magnetometer equipped with a 7 T magnet. The samples were embedded in eicosane to prevent torquing. Diamagnetic corrections were applied to the observed paramagnetic susceptibilities using Pascal's constants.

X-Ray crystallography

Data for a selected crystal of **3**·0.5Et_2O (0.16 × 0.10 × 0.05 mm) were collected at Station 11.3.1 of the Advanced Light Source, at Lawrence Berkeley National Laboratory, using a Bruker AXS Pt200 CCD diffractometer (ω rotation with narrow frames, synchrotron radiation), see Table 1. The structure was solved by direct methods using SHELXS-97[26] and refined on F^2 using full-matrix least-squares with SHELXL-97.[27] All non-H atoms were refined anisotropically. The Et_2O lattice molecule was disorderd by symmetry over two positions and refined with distance and displacement parameter restraints. Also, a pyridyl ring presented some disorder and atoms C1 and C4 were refined with

Table 1 Crystallographic data for complexes **3**·0.5Et_2O and **4**·2MeOH

	3·0.5Et_2O	**4**·2MeOH
Formula[a]	$C_{64}H_{78}Mn_6N_{16}O_{13}Br_4$[b]	$C_{73}H_{82}Mn_8N_{20}O_{33}Cl_4$
M/g mol^{-1} [a]	1928.70	2348.90
Crystal system	Monoclinic	Monoclinic
Space group	$P2_1/c$	$C2/c$
a/Å	12.450(1)	15.225(1)
b/Å	18.147(1)	26.674(1)
c/Å	16.791(1)	23.328(1)
β/°	98.62(1)	107.16(1)
V/Å^3	3750.5(2)	9051.9(4)
Z	2	4
T/K	150(2)	100(2)
λ/Å	0.77490[c]	0.71073[d]
ρ_{calc}/g cm^{-3}	1.708	1.723
μ/mm^{-1}	3.950	1.292
Measd/independent (R_{int}) reflns	39785/11216 (0.0618)	31734/8792 (0.0282)
Obsd reflns [$I > 2\sigma(I)$]	9286	6284
R_1[e]	0.0416	0.0341
wR_2[f]	0.1178	0.0891
GOF on F^2	1.040	1.004
$(\Delta\rho)_{max,min}$/e Å^{-3}	0.991, –0.954	0.717, –0.551

[a] Including solvate molecules. [b] Incorporating the two crystallographically independent molecules. [c] Synchrotron, 'ALS beamline 11.3.1', 'silicon 111' monochromator. [d] Mo-Kα radiation, graphite monochromator. [e] $R_1 = \sum(||F_o| - |F_c||)/\sum(|F_o|)$ for observed reflections. [f] $wR_2 = [\sum[w(F_o^2 - F_c^2)^2]/\sum[w(F_o^2)^2]]^{1/2}$ for all data.

displacement parameter restraints. These still have rather high U_{max}/U_{min} ratios and it was considered to split them, but since this would not add new information, we did not. H atoms were found in difference Fourier maps and placed geometrically on their riding atoms, except those of the Et_2O molecule that could not be found nor fixed. They were nonetheless included in the model and formula.

Data for the selected crystal of **4**·2MeOH (0.28 × 0.15 × 0.14 mm) were collected on an Oxford Diffraction Xcalibur-3 diffractometer (equipped with a Sapphire CCD area detector). Cell parameters were refined by using 15920 reflections ($3.1 \leq \theta \leq 30.2°$). Data (792 frames) were collected using the ω-scan method (0.60° frame). Empirical absorption corrections (multi-scan based on symmetry-related measurements) were applied using CrysAlis RED software.[28] The structure was solved by direct methods using SIR2002[29] and refined on F^2 using full-matrix least-squares with *SHELXL-97*.[27] All non-H atoms were refined anisotropically. Two sets of overlapping positions were defined for four atoms (C29 to C32) of a pyridyl ring and the two orientations were best refined with equal site-occupation factors (50:50); similarity restraints were applied to the bond lengths and atomic displacement parameters of the atoms of each orientation. Restraints were also applied to a ClO_4^- ion (Cl2, O14 to O17) with high displacement parameters to model it to a regular tetrahedron. All H atoms attached to C atoms were positioned geometrically (riding model). The -OH H atom of the lattice MeOH molecule (C37–O9) was located in a difference Fourier map and subsequently refined with a restrained O9–H bond. The programs used were CrysAlis CCD[28] for data collection, CrysAlis RED[28] for cell refinement and data reduction, WINGX[30] and PLATON[31] for crystallographic calculations, and MERCURY[32] and DIAMOND[33] for molecular graphics.

Results and discussion

Syntheses and IR spectra

Many synthetic procedures[19,20,34] to polynuclear Mn clusters rely on the reactions of carboxylate starting materials (either simple Mn^{II} salts such as $Mn(O_2CR')_2$ (R′ = various), or preformed higher oxidation Mn_x carboxylate clusters such as $[Mn_3O(O_2CR')_6L_3]^{0/+}$ [35] or $[Mn^{III}_4O_2(O_2CPh)_9(H_2O)]^-$ [36]) with a potentially chelating/bridging ligand. Both routes were known from our previous work to yield magnetically and structurally interesting complexes upon reaction with mpkoH.[19] In the present study we have investigated the reactions with two simple Mn^{II} sources, *i.e.* $MnBr_2$ and $Mn(ClO_4)_2·6H_2O$, *in the absence of carboxylate groups.*

The 1:1 reaction between $MnBr_2$ and mpkoH in MeOH in the presence of one equivalent of OH^- gave $[Mn_3(OMe)_2(mpko)_4Br_2]$ (**3**), a mixed-valent $Mn^{II}_2Mn^{IV}$ species; the Mn^{IV} ion clearly was formed by aerial oxidation of Mn^{II} in the presence of the base. At first sight, it is rather surprising that the hard Mn^{IV} center is not coordinated to O^{2-} ions,[37] but it is well known that the oximate group can stabilize higher metal oxidation states.[18i,21,38] Given the rather low isolated yield of **3**, the presence of other species in the filtrate is probable, but we have not explored this further. As with many reactions in higher oxidation state Mn chemistry, it is likely that the solution contains a mixture of several species in equilibrium, and what crystallizes out is determined by relative solubilities, the nature of any counterions, lattice energies, and related factors.[9g] In the present case, this is supported by the isolation of complex **4** when non-coordinating ClO_4^- ions were used in place of the coordinating Br^- ions. However, the complexes $[Mn^{II}_2Mn^{IV}(OMe)_2(mpko)_4X_2]$ ($X^- = Cl^-$, SCN^-, NCO^-), analogous to **3**, were obtained when these X^- groups were used in place of Br^-.

The 1:2 reaction between $Mn(ClO_4)_2·6H_2O$ and mpkoH in the presence of one equivalent of OH^- in MeOH gives the complex $[Mn^{II}_2Mn^{III}_6O_4(OMe)(mpko)_9(mpkoH)](ClO_4)_4$ (**4**). The excess of mpkoH is beneficial to the yield (~60%); the same product, but with a lower yield, is isolated from 1:1:1 $Mn(ClO_4)_2·6H_2O$/mpkoH/OH^- reaction mixtures. Prolonged solvent evaporation should be avoided otherwise the product crystals are contaminated with $LiClO_4$, requiring copious washing with MeOH to obtain an analytically pure sample. It is interesting that although the average Mn oxidation states of **3** and **4** (+2.67 *vs.* +2.75, respectively) and their $mpko^-$:Mn ratio (1.33 *vs.* 1.25) are very similar, the two products have very different nuclearities and structures.

The presence of neutral oxime group(s) in a vacuum-dried, *i.e.*, lattice MeOH-free, sample of **4** is manifested by a broad IR band of medium intensity at 3438 cm^{-1}, assigned to $\nu(OH)_{oxime}$;[39] its broadness is indicative of hydrogen-bonding. This band is also present in the hexachlorobutadiene mull spectrum of this compound at ~3410 cm^{-1}. The in-plane deformation of the 2-pyridyl ring of free mpkoH at 632 cm^{-1} shifts upwards in **3** (638 cm^{-1}) and **4** (660 cm^{-1}) confirming the involvement of the ring N-atom in coordination.[40] Several bands appear in the 1600–1400 cm^{-1} region in the spectra of the two complexes. Contributions from the $\nu(C{=}N)_{oximate}$ and $\delta(CH_3)$ modes would be expected in this region, but overlap with the stretching vibrations of the aromatic ring renders assignments

This journal is © The Royal Society of Chemistry 2009

and discussion of the coordination shifts difficult. The medium band at 1116 cm^{-1} in the spectrum of free mpkoH was previously assigned to the $\nu(NO)_{oxime}$ mode.[41] The frequency of this vibration has increased to 1138 cm^{-1} in **3** and to 1146 cm^{-1} in **4**. This shift to higher frequencies has been discussed, and is in accord with the concept that upon deprotonation and oximate-O coordination there is a higher contribution of N=O to the electronic structure of the oximate group; consequently the ν(NO) vibration shifts to a higher frequency in the complexes relative to mpkoH.[41] A medium intensity band at 587 cm^{-1} is present in the IR spectrum of **4**; this band is absent from the spectrum of **3** and can be assigned[42] to a vibration involving a Mn^{III}–O^{2-} stretch. The spectrum of **4** exhibits strong bands at 1092 and 622 cm^{-1}, due to the $\nu_3(F_2)[\nu_d(ClO)]$ and $\nu_4(F_2)[\delta_d(OClO)]$ modes, respectively, of the uncoordinated T_d ClO_4^- ions;[43] the broad character and splitting of the band at ~1090 cm^{-1} indicates the involvement of ClO_4^- ions in hydrogen bonding.

Description of structures

$[Mn_3(OMe)_2(mpko)_4Br_2]\cdot 0.5Et_2O$ (**3**·0.5Et_2O) crystallizes in the monoclinic space group $P2_1/c$. There are two crystallographically independent molecules in the unit cell, but their interatomic distances and angles differ only marginally. Thus, only one (that containing Mn1 and Mn2) will be discussed in detail. A partially labelled plot of this molecule is shown in Fig. 1, while selected interatomic distances and angles are listed in Table 2.

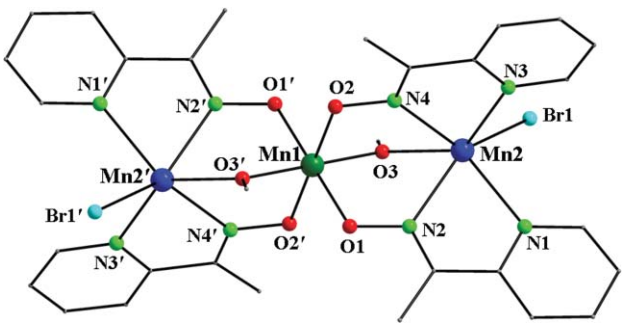

Fig. 1 Partially labelled plot of one of the two crystallographically independent molecules in **3**·0.5Et_2O. Colour scheme: Mn^{II}, blue; Mn^{IV}, dark green; O, red; N, green; C, gray; Br, sky blue. Primed and unprimed atoms are related by the crystallographic inversion centre.

Central atom Mn1 is located on a crystallographic inversion center and is coordinated by four $\eta^1{:}\eta^1{:}\eta^1{:}\mu$-mpko$^-$ O atoms and two μ-OMe groups (O3, O3′). Atoms Mn2 and Mn2′ are each coordinated by four nitrogen atoms belonging to the 'chelate' part of two mpko$^-$ ligands, one Br^- ion, and one μ-OMe group. Charge considerations require formal $2Mn^{II}$, Mn^{IV} or Mn^{II}, $2Mn^{III}$ descriptions. The terminal Mn atoms are clearly high-spin Mn^{II} based on their Mn–O and Mn–N bond lengths (all >2.185 Å), which are typical for Mn(II) complexes with N,O-ligation.[39a] The central Mn1 has short Mn–O distances in the range 1.893(2)–1.912(2) Å;[37,38c] this, and the absence of a Jahn–Teller (JT) axial elongation that would be expected for a high-spin, $3d^4$ Mn^{III} ion in near octahedral geometry, indicate that Mn1 is a Mn^{IV} atom. These Mn oxidation states were confirmed by bond valence sum (BVS) calculations,[44] which give values of 4.23 and 1.99 for Mn1 and Mn2, respectively; the corresponding values for the other crystallographically independent Mn_3 molecule are 4.16 and 2.08 for Mn4 and Mn3, respectively. BVS calculations also confirm that O3 and O3′ (and O6 and O6′ in the second Mn_3 molecule) are MeO^- groups, the BVS values being 1.88 and 1.94, respectively. The coordination environments around the metal centers are consistent with the HSAB principle; the environment around the Mn^{II} atoms consists of the N_4OBr donor atoms set, while Mn^{IV} possesses an O_6 set.

Table 2 Selected interatomic distances (Å) and angles (°) for one[a] of the crystallographically independent trinuclear molecules of complex **3**·0.5Et_2O

Mn1 ··· Mn2	3.415(1)	Mn2–N1	2.319(2)
Mn2 ··· Mn2′[b]	6.829(2)	Mn2–N2	2.248(2)
Mn1–O1	1.910(2)	Mn2–N3	2.302(2)
Mn1–O2	1.912(2)	Mn2–N4	2.273(2)
Mn1–O3	1.893(2)	Mn2–Br1	2.565(1)
Mn2–O3	2.185(2)		
O1–Mn1–O2	91.1(1)	N1–Mn2–N4	128.2(1)
O1–Mn1–O3	91.5(1)	N1–Mn2–Br1	93.9(1)
O2–Mn1–O3	91.0(1)	N2–Mn2–N3	118.3(1)
O3–Mn2–N1	130.8(1)	N2–Mn2–N4	79.4(1)
O3–Mn2–N2	75.7(1)	N2–Mn2–Br1	143.7(1)
O3–Mn2–N3	137.9(1)	N3–Mn2–N4	69.3(1)
O3–Mn2–N4	75.6(1)	N3–Mn2–Br1	92.7(1)
O3–Mn2–Br1	94.2(1)	N4–Mn2–Br1	132.5(1)
N1–Mn2–N2	69.6(1)	Mn1–O3–Mn2	113.5(1)
N1–Mn2–N3	90.0(1)		

[a] This is the molecule shown in Fig. 1. [b] Symmetry code: (′) = −*x*, −*y*, −*z*.

The Mn1 polyhedron is almost a perfect octahedron. The Mn1–O(1,2,3) distances and the *cis* O–Mn1–O bond angles are in the narrow ranges 1.893(2)–1.912(2) Å and 88.5(1)–91.5(1), respectively. The Mn^{II} ion is distorted trigonal prismatic (Fig. 2): One N atom of each of the mpko$^-$ ligands and the methoxo O atom or the bromide ion constitute the two trigonal faces. The lengths of the triangular faces are in the range 2.720(3)–2.888(3) Å for the triangle N2–N4–O3 and 3.266(3)–3.572(2) Å for the triangle N1–N3–Br1, and all angles are in the range 54.8(1)–64.0(1)°. The two trigonal faces are not parallel, the planes defined by N1–N3–Br1 and N2–N4–O3 making an angle of 17.5(1)°. The four mpko$^-$ N atoms make up a distorted rectangle, while the remaining two tetragonal faces are irregular trapezoids. Mixed-ligand, high-spin Mn(II) complexes with a trigonal prismatic coordination geometry have been reported and discussed.[45] Note

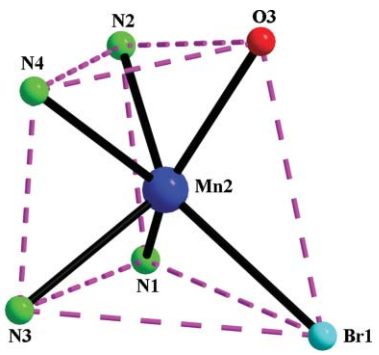

Fig. 2 The distorted trigonal prismatic geometry of Mn2 in complex **3**. Colour scheme as in Fig. 1.

that for the high-spin d^5 six-coordination, the octahedron is not preferred by both VSEPR/steric and dσ* occupation factors.[46]

The reason for two inequivalent Mn_3 molecules in the unit cell appears to be the solvate Et_2O molecule. The compound is $\{[Mn_3(OMe)_2(mpko)_4Br_2]\}\{[Mn_3(OMe)_2(mpko)_4Br_2]\cdot Et_2O\}$: molecule A (that shown in Fig. 1) is 'bare', whereas molecule B contains the lattice Et_2O molecule in a cavity formed by four $mpko^-$ ligands from two, symmetry-related B molecules. The latter form 1D chains (Fig. 3) that are separated by molecules of type A that do not display significant intermolecular interactions. The Et_2O molecules are tightly 'locked' within the cavities, and as a result the crystals do not degrade in air on removal from mother liquor, unlike the usual situation when crystals containing solvate Et_2O molecules are allowed to dry; complex **3** analyzes as Et_2O-free only after drying in *vacuo*. A significant consequence of the $[Mn_3(OMe)_2(mpko)_4Br_2]/Et_2O$ interaction is the increase of the Mn^{II}–N–O–Mn^{IV} torsion angles in the molecules of type B by 10.1 and 14.0° compared with those in the 'bare' Mn_3 molecules A.

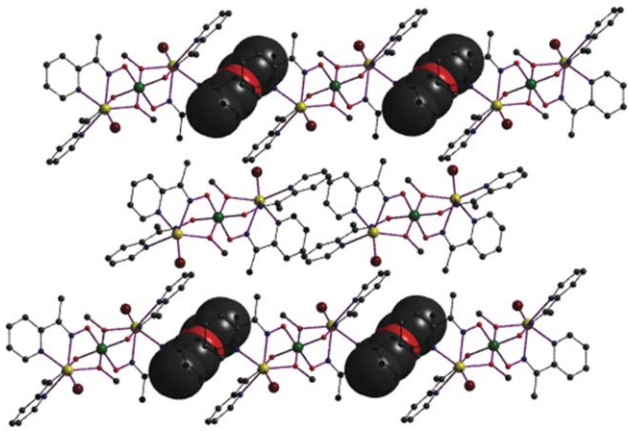

Fig. 3 Portions of two 1D chains $\{[Mn_3(OMe)_2(mpko)_4Br_2]\cdot Et_2O\}$ separated by one array of 'bare' $[Mn_3(OMe)_2(mpko)_4Br_2]$ for complex **3**·0.5Et_2O.

Complex **3** joins a rather large family of non-triangular, mixed-valence Mn_3 complexes. Most of them have only a one-unit difference in Mn oxidation state, *i.e.* $Mn^{II}_2Mn^{III}$,[47,48] $Mn^{II}Mn^{III}_2$[47,49] and $Mn^{V}Mn^{VI}_2$.[50] Complex **3** is thus rare in joining only a handful of Mn_3 complexes with a two-unit difference between oxidation states, the previous $Mn^{II}_2Mn^{IV}$ examples also containing a 2-pyridyl oximate ligand.[51] A remarkable, non-triangular $Mn^{III}Mn^{II}Mn^{IV}$ complex with a 2-aminophenol-based non-innocent ligand has also been reported.[52] Tetranuclear $Mn^{II}_2Mn^{IV}_2$[53a] and $Mn^{II}_3Mn^{IV}$,[53b,c] complexes are also known.

Complex **4**·2MeOH crystallizes in the monoclinic space group $C2/c$. Its structure consists of octanuclear $[Mn_8O_4(OMe)(mpko)_9(mpkoH)]^{4+}$ cations, ClO_4^- anions and solvate MeOH molecules in an 1:4:2 ratio. The hydroxyl group of the lattice MeOH molecule (O9) is hydrogen-bonded to the O atom of one ClO_4^- ion (O14): O9···O14 2.766(5) Å, H(O9)···O(14) 1.847(10) Å, O9H(O9)O(14) = 168(5)°. The partially labelled structure of the cation of complex **4**·2MeOH is shown in Fig. 4 and two views of its core are illustrated in Fig. 5. Selected interatomic distances and angles are listed in Table 3.

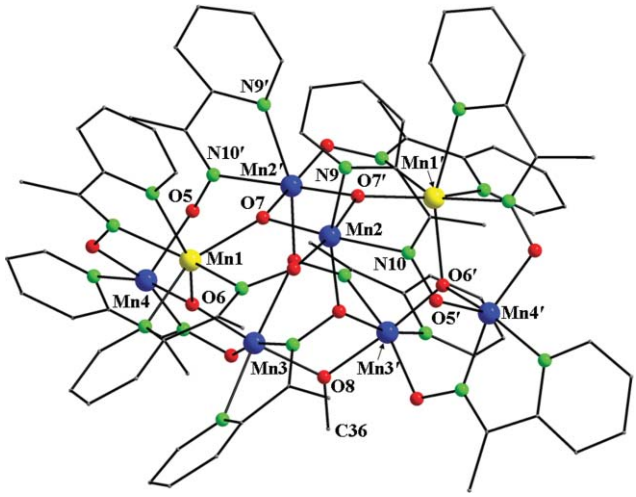

Fig. 4 Partially labelled plot of the cation of complex **4**·2MeOH. Colour scheme: Mn^{II}, yellow; Mn^{III}, blue; O, red; N, green; C, gray. Primed and unprimed atoms are related by the crystallographic two-fold axis.

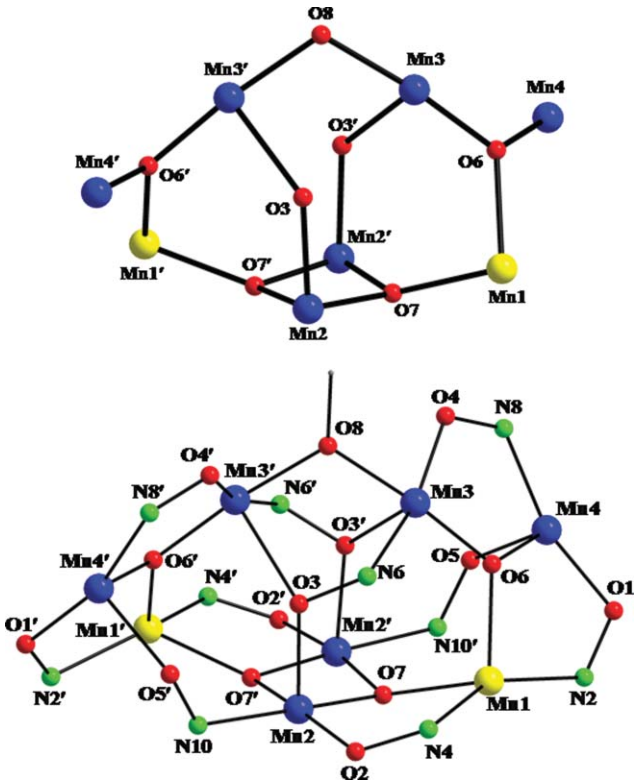

Fig. 5 The $[Mn^{II}_2Mn^{III}_6(\mu_3\text{-}O)_4(\mu\text{-}OMe)(\mu\text{-}OR'')_2]^{11+}$ core of **4** (top) and a more detailed representation emphasizing its $[Mn^{II}_2\text{-}Mn^{III}_6(\mu_3\text{-}O)_4(\mu\text{-}OMe)(\mu\text{-}OR'')_2(\mu\text{-}ONR''')_7(\mu\text{-}HONR''')]^{4+}$ description. Colour scheme as in Fig. 4. O6, O6′, O7, O7′ are the oxide atoms, while O1, O2, O3, O4, O5, N2, N4, N6, N8, N10 and their symmetry equivalents belong to the oximate groups of the $mpko^-$ ligands; atom O8 belongs to the bridging methoxide group.

The cation of **4** lies on a two-fold rotation axis (C_2) passing through atoms O8 and C36. The metal ions are held together by four $\mu_3\text{-}O^{2-}$ ions (O6, O6′, O7, O7′), one μ-MeO^- group

 This journal is © The Royal Society of Chemistry 2009

Table 3 Selected interatomic distances (Å) and angles (°) for complex **4**·2MeOH[a]

Mn1 ··· Mn2	3.453(1)	Mn2–O7	1.868(2)
Mn1 ··· Mn2′	3.584(1)	Mn2–O7′	1.867(2)
Mn1 ··· Mn3	3.469(1)	Mn2–N9	2.161(2)
Mn1 ··· Mn4	3.399(1)	Mn2–N10	2.122(2)
Mn2 ··· Mn2′	2.827(1)	Mn3–O3′	2.281(2)
Mn2 ··· Mn3	4.255(1)	Mn3–O4	1.916(2)
Mn2 ··· Mn4	5.849(1)	Mn3–O6	1.846(2)
Mn3 ··· Mn3′	3.226(1)	Mn3–O8	1.943(2)
Mn3 ··· Mn4	3.126(1)	Mn3–N5	2.261(2)
Mn1–O6	2.127(2)	Mn3–N6	2.037(2)
Mn1–O7	2.065(2)	Mn4–O1	1.885(2)
Mn1–N1	2.320(2)	Mn4–O5	2.093(2)
Mn1–N2	2.244(2)	Mn4–O6	1.842(2)
Mn1–N3	2.220(2)	Mn4–N7	2.053(2)
Mn1–N4	2.262(2)	Mn4–N8	1.989(2)
Mn2–O2	1.940(2)	Mn4 ··· O10[b]	2.687(2)
Mn2–O3	2.063(2)		
O6–Mn1–N1	151.0(1)	O6–Mn4–N7	164.3(1)
O7–Mn1–N3	149.4(1)	Mn1–O6–Mn3	121.5(1)
N2–Mn1–N4	152.7(1)	Mn1–O6–Mn4	117.6(1)
O2–Mn2–O7′	171.7(1)	Mn3–O6–Mn4	115.9(1)
O3–Mn2–N9	160.3(1)	Mn1–O7–Mn2	122.7(1)
O7–Mn2–N10	176.2(1)	Mn1–O7–Mn2′	131.4(1)
O3′–Mn3–N5	165.4(1)	Mn2–O7–Mn2′	98.4(1)
O4–Mn3–N6	165.7(1)	Mn2–O3′–Mn3	129.4(1)
O6–Mn3–O8	174.1(1)	Mn3–O8–Mn3′	112.2(1)
O1–Mn4–N8	163.1(1)		

[a] Symmetry code: (′) = $-x$, y, $1/2 - z$. [b] O10 is in a ClO_4^- ion not shown in Fig. 4.

Table 4 Bond valence sum (BVS)[a] calculations for the Mn and selected O atoms in **4**

Atom	Mn^{II}	Mn^{III}	Mn^{IV}
Mn1	**2.00**	1.86	1.90
Mn2	3.50	**3.25**	3.33
Mn3	3.27	**3.03**	3.11
Mn4	3.21	**3.00**	3.04
Atom	BVS	Assignment	
O6	1.77	O^{2-}[b]	
O7	1.74	O^{2-}[b]	
O8	1.97	MeO^-[c]	

[a] The value in bold is the one closest to the charge for which it was calculated. The oxidation state is the nearest whole number to the bold value. [b] An O BVS in the ~1.8–2.0, ~1.0-1.2 and ~0.2–0.4 ranges is indicative of non-, single- and double-protonation, respectively. [c] Values of ~2 and ~1 are indicative of methoxide ions and neutral MeOH molecule, respectively.

(O8), eight $\eta^1{:}\eta^1{:}\eta^1{:}\mu$ and two (O3 and O3′) $\eta^1{:}\eta^1{:}\eta^2{:}\mu_3$ oximate ligands to give a $[Mn_8(\mu_3\text{-}O)_4(\mu\text{-}OMe)(\mu\text{-}OR'')_2]^{11+}$ core [R″ = (py)C(Me)N; Fig. 5, top]. Peripheral ligation is provided by ten pairs of nitrogen atoms that belong to the 'chelating' parts of the organic ligands and eight terminally ligated oximate oxygen atoms (O1, O2, O4, O5 and their symmetry equivalents). If we consider the bridging diatomic oximate groups as part of the core, then the latter becomes $[Mn_8(\mu_3\text{-}O)_4(\mu\text{-}OMe)(\mu\text{-}OR'')_2(\mu\text{-}ONR''')_7(\mu\text{-}HONR''')]^{4+}$; this view is emphasized in Fig. 5 (bottom). Atoms Mn1, Mn2 and Mn3 are six-coordinate with distorted octahedral geometry. In contrast, Mn4 is five-coordinate: analysis of its shape-determining angles using the approach of Addison, Reedijk *et al.*[54] yields a value for the trigonality index, τ, of 0.02 (τ = 0 and 1 for perfect spy and tbp geometries, respectively; spy = square pyramidal, tbp = trigonal bipyramidal). Thus, the geometry about Mn4 is square pyramidal with the oximate oxygen atom O5 at the apical position. Mn4 is 2.687(2) Å from a ClO_4^- atom O10; this distance represents only a very weak bonding interaction at best, and we thus prefer the formulation of the Mn_8 unit as a tetracation. Of the four pairs of $\eta^1{:}\eta^1{:}\eta^1{:}\mu$ organic ligands, the pair with atoms N9, N10 and O5′ [and its symmetry equivalent] deserve some comment: these ligands are in the *syn,anti* conformation, which is rare in transition metal oximate complexes.[22] This results in a very large value (87.3°) for the Mn2–N10–O5′–Mn4′ torsion angle.

The Mn oxidation states of **4** are obvious from the metric parameters (Table 3), BVS calculations[44] (Table 4), and the clear presence of JT axial elongations at Mn2 and Mn3. Thus, Mn1 is a Mn^{II} atom, and Mn2, Mn3 and Mn4 are Mn^{III} atoms, giving an overall $Mn^{II}_2Mn^{III}_6$ description. As is almost always the case, the JT elongation axes avoid the Mn^{III}–O^{2-} bonds, the shortest and strongest in the cation.[55] Atoms O6 and O7 were confirmed as O^{2-} ions by BVS calculations (Table 4).[44] Thus the cation initially appeared to be $[Mn^{II}_2Mn^{III}_6O_4(MeOH)(mpko)_{10}]^{4+}$, its tetracationic nature agreeing with the four observed ClO_4^- anions. However, we were unhappy with this formula, because there is no literature precedent for MeOH groups bridging two Mn^{III} atoms; the high Lewis acidity of the latter should make the MeOH molecule in a $[Mn^{III}_2(\mu\text{-}OHMe)]$ unit very (Brønsted) acidic (very low pk_a) and unlikely to be stable. In addition, the Mn3-O8 bond length (1.943(2) Å) is typical of Mn^{III}-μ-OMe^- bond lengths.[20] We thus concluded that O8 is part of a bridging MeO^- group, and this was confirmed by the O8 BVS of 1.97, confirming it as deprotonated; MeO^- is a more realistic bridging group between two Mn^{III} atoms.[56] To maintain the 4+ charge of the cation, it is very likely that the C_2 symmetry axis is masking the presence of a proton statically disordered between a $mpko^-$/mpkoH pair, or even among several such groups. We thus formulate the cation as $[Mn_8O_4(OMe)(mpko)_9(mpkoH)]^{4+}$. A static disorder of an H^+ over two or more sites would average out its influence on the structural parameters and thus make it very difficult to detect. Nevertheless, we have calculated the BVS values of the oximate O atoms, and obtained 1.60, 1.53, 1.55, 1.60 and 1.40 for O1, O2, O3, O4 and O5, respectively. None of these are values expected for a 100% protonated O atom, but the somewhat smaller value for O5 compared to the others might be indicative of protonation, remembering also that there are two symmetry-related O5 atoms and only one putative H^+ so the level of protonation would be 50% at most, and that in any case the H^+ could also be partially disordered over the other O atoms as well. Note that the O5 ··· O3 (2.855 Å) is consistent with a (50%) hydrogen-bond. It should also be recalled (see the IR discussion) that the vacuum-dried, solvent-free sample of **4** exhibits an IR band (KBr, hexachlorobutadiene) at ~3420 cm^{-1} assignable to the $\nu(OH)_{oxime}$ mode.[39]

The Mn_8 topology of **4** (Fig. 5, top) can be described in two ways: (i) as a $\{Mn^{II}_2Mn^{III}_2(\mu_3\text{-}O)_2\}^{6+}$ butterfly unit (Mn1, Mn1′, Mn2, Mn2′, O7, O7′) bridged to four additional Mn^{III} atoms by oxide atoms O6 and O6′ and oximate atoms O3 and O3′, giving a 'triangle-butterfly-triangle' description; and (ii) as a U-shaped sequence of four fused $\{Mn_3(\mu_3\text{-}O)\}^{6+}$ triangular units sharing either a vertex or an edge (Fig. 6).

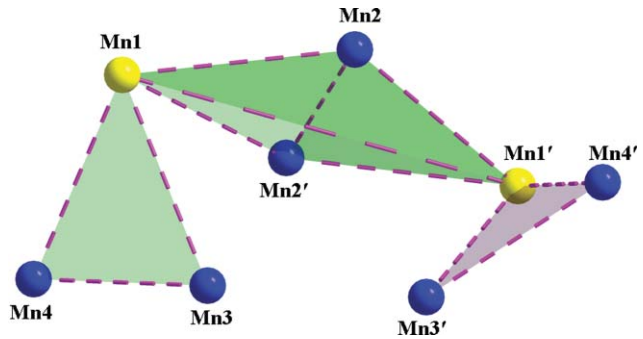

Fig. 6 The metallic skeleton of **4** emphasizing the fused 'triangle-butterfly-triangle' and 'four triangles' metal topologies.

Complex **4** joins a family of Mn clusters of nuclearity eight, which currently comprise the metal oxidation levels Mn^{II}_8,[57] $Mn^{II}_6Mn^{III}_2$,[9g,12b,58] $Mn^{II}_4Mn^{III}_4$,[13,14a,16d,19e,39a,59] $Mn^{II}_2Mn^{III}_6$,[9c,9f,20a,36,60] Mn^{III}_8[4b,34a,61] and $Mn^{III}_2Mn^{IV}_6$[62] (only representative examples are given) and thus becomes a member of the $Mn^{II}_2Mn^{III}_6$ subfamily. The octanuclear Mn clusters possess a variety of metal topologies such as rodlike, serpentine, rectangular, linked butterfly units, linked tetrahedral, edge-sharing cubane units with an additional Mn ion *etc.*, but none have possessed the core of **4**.

Complexes **3** and **4** are members of a relatively small family of Mn complexes with deprotonated 2-pyridyl oximes,[16d,18,19,21c,39a,51,53b,53c,63] and pyridyl dioximes[20] as ligands (Scheme 1).

Magnetochemistry

Variable-temperature dc magnetic susceptibility studies were performed on powdered samples of compounds **3** and **4**, restrained in eicosane to prevent torquing, in an applied dc field of 0.1 T (1.0 kG) and in the 5.0–300 K range.

$\chi_M T$ for **3** steadily increases from 11.81 cm^3 K mol^{-1} at 300 K to a maximum of 19.71 cm^3 K mol^{-1} at 8 K, and then drops sharply to 18.90 cm^3 K mol^{-1} at 5.0 K (Fig. 7). The 300 K value is larger than the 10.63 cm^3 K mol^{-1} value expected for two Mn^{II} and one Mn^{IV} non-interacting ions with $g = 2$, indicating the presence of dominant ferromagnetic exchange interactions and a probable $S = 13/2$ ground state. The decrease in $\chi_M T$ at the lowest temperatures is likely due to zero-field splitting (ZFS), Zeeman effects from the applied field, and perhaps some weak intermolecular antiferromagnetic interactions.

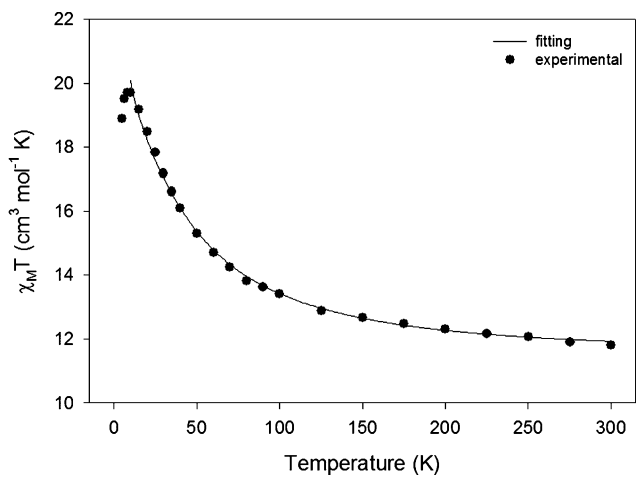

Fig. 7 Plot $\chi_M T$ *vs.* T for a powdered sample of complex **3**. The solid line is the fit of the data; see the text for the fit parameters.

The isotropic Heisenberg spin Hamiltonian appropriate for the centrosymmetric complex **3** is given by eqn (1), where S_i refers to the spin of atom Mn_i in Fig. 1. Thus $J = J_{12} = J_{12'}$ and

$$\mathscr{H} = -2J(\hat{S}_1 \cdot \hat{S}_2 + \hat{S}_1 \cdot \hat{S}_{2'}) - 2J'\hat{S}_2 \cdot \hat{S}_{2'} \quad (1)$$

$J' = J_{22'}$. Application of the Kambe method,[64] using the substitutions $\hat{S}_A = \hat{S}_2 + \hat{S}_{2'}$ and $\hat{S}_T = \hat{S}_A + \hat{S}_1$ (where S_T is the total spin of the molecule), gives the equivalent spin Hamiltonian of eqn (2).

$$\mathscr{H} = -J(\hat{S}_T{}^2 - \hat{S}_A{}^2 - \hat{S}_1{}^2) - J'(\hat{S}_A{}^2 - \hat{S}_2{}^2 - \hat{S}_{2'}{}^2) \quad (2)$$

The eigenvalues of eqn (2) are given by eqn (3), where $E(S_T, S_A)$ is the energy of state S_T arising from S_A, and constant terms contributing to all states have been omitted.

$$E(S_T, S_A) = -J[S_T(S_T + 1) - S_A(S_A + 1)] - J'[S_A(S_A + 1)] \quad (3)$$

For complex **3**, $S_1 = 3/2$, $S_2 = S_{2'} = 5/2$, and the overall multiplicity of the spin system is 144, made up of 20 individual spin states ranging from $S_T = 1/2$ to 13/2. A theoretical $\chi_M T$ *vs.* T expression was derived using the S_T values, their energies $E(S_T)$ and the Van Vleck equation, and this expression was used to fit the experimental data. Data below 8 K were omitted because the low-temperature decrease of $\chi_M T$ is caused by factors not included in the above model. The fit parameters were J, J' and g. A temperature-independent paramagnetism (TIP) term was included, held fixed at 600×10^{-6} cm^3 mol^{-1}. A good fit was obtained for **3** (solid line in Fig. 7) with the fit parameters $J = +3.4(1)$ cm^{-1}, $J' = +0.3(2)$ cm^{-1} and $g = 2.00(2)$. Since **3**·0.5 Et_2O consists of two crystallographically independent (but structurally very similar) trinuclear molecules, the values for the fit parameters may be considered as the average. However, since the crystals have been crushed and the sample used for the magnetic study has been analysed as Et_2O-free, the fit parameters can be considered as real values from the two molecules that have now converged to a similar structure. A fit of the data to a 1-J model (*i.e.*, $J' = 0$) gave poor results and a g value significantly greater than 2.0, suggesting that the long $Mn^{II} \cdots Mn^{II}$ exchange interaction cannot be ignored. The exchange interactions in **3** are thus weakly ferromagnetic, giving an $S_T = 13/2$ ground state, the $|S_T, S_A> = |13/2, 5>$ state. The first excited state is $|S_T, S_A> = |11/2, 4>$ at 13.27 cm^{-1} above the ground state.

To obtain the zero-field splitting parameter D, magnetization *vs.* dc field measurements were made on a restrained sample of **3** at applied fields and temperatures in the 1.0–6.0 T and 1.8–10.0 K ranges, respectively. The resulting data are shown in Fig. 8 as a reduced magnetization ($M/N\mu_B$) *vs.* H/T plot, where M is the magnetization, N is Avogadro's number, μ_B is the Bohr magneton, and H is the magnetic field. The data were fit using the program MAGNET[65] to a model that assumes that only the ground state is populated at these temperatures and magnetic fields, includes isotropic Zeeman interactions and axial zero-field splitting ($D\hat{S}_z{}^2$), and incorporates a full powder average. The corresponding spin

 This journal is © The Royal Society of Chemistry 2009

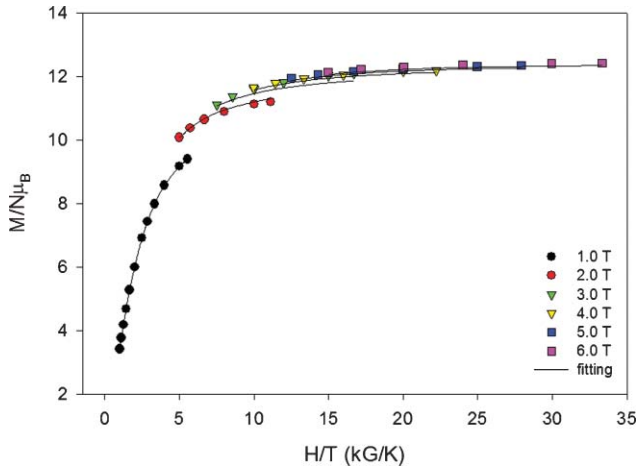

Fig. 8 Plot of reduced magnetization ($M/N\mu_B$) *vs.* H/T for complex **3**. The solid lines are the fits of the data for a positive D value; see the text for the fit parameters.

Hamiltonian is given by eqn (4), where $\hat{S}_z$ is the easy-axis spin operator and μ_0 is the vacuum permeability.

$$\mathscr{H} = D\hat{S}_z^2 + g\mu_B\mu_0\hat{S}\cdot H \quad (4)$$

The last term in eqn (4) is the Zeeman energy associated with an applied magnetic field. The various isofields lines do not superimpose, indicating significant ZFS in the ground state. The best fit for **3** is shown as the solid lines in Fig. 8 and was obtained with $S = 13/2$ and either of the two sets of parameters: $g = 1.93$, $D = -0.15$ cm^{-1} and $g = 1.92$, $D = +0.17$ cm^{-1}. Alternative fits with $S = 11/2$ or smaller were rejected because they gave unreasonable values of g and D. Since magnetization fits are not particularly sensitive to the sign of D, often one obtains two acceptable fits of magnetization data for a given S value, one with $D > 0$ and the other with $D < 0$. In order to assess which is the superior fit and also to ensure that the true global minimum had been located, we calculated the root-mean-square D *vs.* g error surface using the program GRID[66] which calculates the relative difference between the experimental $M/N\mu_B$ data and those calculated for various combinations of g and D. The error surface, plotted as a two-dimensional contour plot in Fig. 9 shows only the two minima with positive and negative D values, with the former being of superior quality, thus suggesting that the true sign of D is positive.

As we have reported before on many occasions,[67] ac magnetic susceptibility studies are a good complement to dc studies for the determination of the ground state of a cluster, because they preclude any complications from the presence of a dc field. We thus carried out ac studies on **3** as an independent determination its ground state spin. These were performed in the 1.8–15 K range using a 3.5 G ac field oscillating at frequencies in the 50–1000 Hz range. Fig. 10 shows the in-phase component χ'_M of the ac susceptibility, plotted as $\chi'_M T$ *vs.* T. $\chi'_M T$ is slightly increasing below 15 K indicating depopulation of excited states with S smaller than that of the ground state, and extrapolation of the plot to 0 K from above 8 K (to avoid the decrease at the lowest T due to weak intermolecular interactions, anisotropy, *etc.*) gives a value of just over 22 cm^3 K mol^{-1}. This indicates an $S = 13/2$ ground state and g slightly less than 2.0, in agreement with the dc magnetization fit. Complex **3** does not exhibit an out-of- phase ac susceptibility signal down to 1.8 K (Fig. S1 in the ESI†), confirming it is not a SMM. This was expected due to the positive D value.

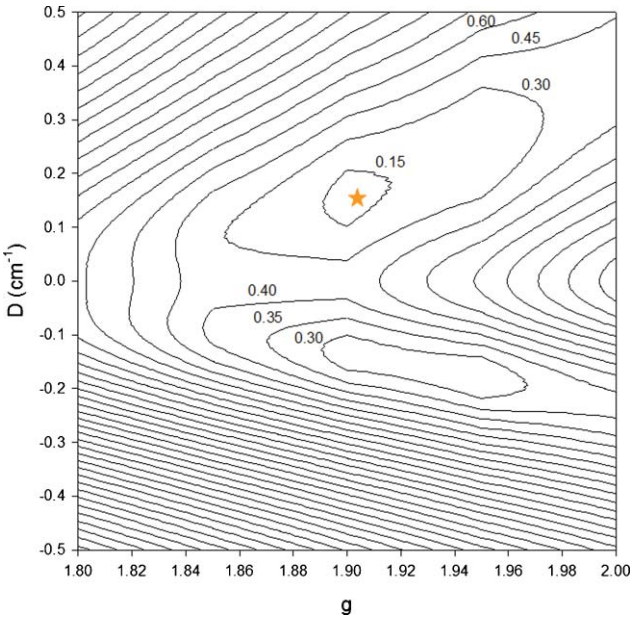

Fig. 9 Two-dimensional contour plot of the root-mean-square error surface for the D *vs.* g fit for complex **3**. The asterisk indicates the error minimum.

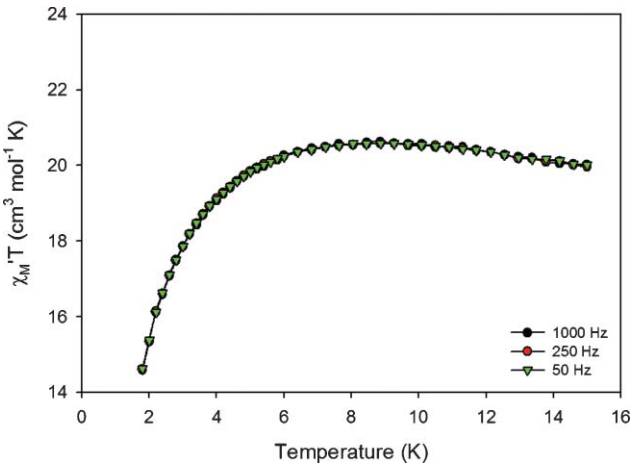

Fig. 10 Plot of $\chi'_M T$ *vs.* T for complex **3** at the indicated frequencies.

The obtained J value for the $Mn^{IV}\cdots Mn^{II}$ interaction in **3** (+3.4 cm^{-1}) is similar to those (+3.1 to +4.1 cm^{-1}) for the structurally similar complexes $[Mn_3(OMe)_2(ppko)_4X_2]$[51] [ppko$^-$ is the anion of di-2-pyridyl ketone oxime (Scheme 1), and X$^-$ is SCN$^-$, OCN$^-$, and Cl$^-$]; for these complexes, the $Mn^{II}\cdots Mn^{II}$ exchange interaction was not included in the fitting, and no D values were provided. In general, $Mn^{IV}\cdots Mn^{II}$ exchange interactions reported in the literature have ranged from weakly ferromagnetic[51] (J = +3.1 to +4.1 cm^{-1}) to very weak[53b,53c] (J = –0.3 to –1.8 cm^{-1}) and moderate[53a,53e] (J = –24.2, –26.8 cm^{-1}) antiferromagnetic ones; the sign of the interaction depends on the metal topology.

$\chi_M T$ for **4** decreases from 17.84 cm^3 K mol^{-1} at 300 K to 9.79 cm^3 K mol^{-1} at 50 K, before decreasing rapidly below 20 K

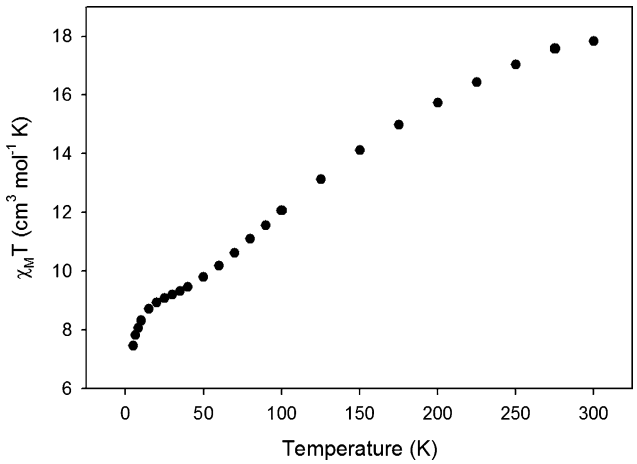

Fig. 11 Plot $\chi_M T$ *vs.* T for a powdered sample of complex **4**.

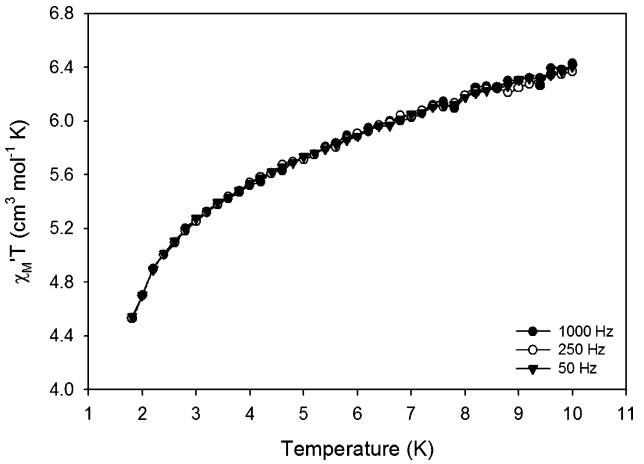

Fig. 13 Plot of $\chi'_M T$ *vs.* T for complex **4** at the indicated frequencies.

to a value of 7.40 cm^3 K mol^{-1} at 5.0 K (Fig. 11). This behaviour indicates the presence of dominant antiferromagnetic exchange interactions and a low, but nonzero, ground state S value. The 300 K value is significantly lower than the spin-only ($g = 2$) value of 27.75 cm^3 K mol^{-1} for two Mn^{II} and six Mn^{III} non-interacting ions. The $\chi_M T$ value at 5.0 K is approaching that for an $S = 3$ ground state, for which the spin-only ($g = 2$) value is 6.0 cm^3 K mol^{-1}. Given the size of the Mn_8 cation, and the resulting number of inequivalent exchange constants, it is not possible to apply the Kambe method.[64]

In order to determine the ground state S and the ZFS parameter, D, M *vs.* H data were collected in the field and temperature ranges 0.1–1.0 T and 1.8–10.0 K, respectively, and plotted as $M/N\mu_B$ *vs.* H/T in Fig. 12. The data were fit as described for complex **3**; we used only low field data ($\leq$1.0 T) to preclude problems from low-lying excited states, which are expected for high-nuclearity clusters with a high density of spin states and/or when Mn^{II} ions are present, which give weak exchange interactions.[68] The best fit is shown as the solid lines in Fig. 12 and was obtained with $S = 3$, $g = 1.99$ and $D = -0.09$ cm^{-1}.

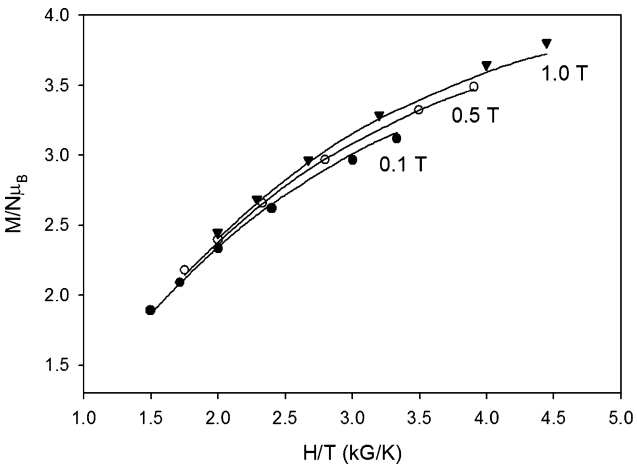

Fig. 12 Plot of reduced magnetization ($M/N\mu_B$) *vs.* H/T for complex **4**. The solid lines are the fits of the data; see the text for the fit parameters.

We also performed ac susceptibility measurements in a 3.5 G ac field oscillating at frequencies in the 50–1000 Hz range as an additional and independent means to confirm the ground state spin. The in-phase $\chi'_M T$ *vs.* T data are shown in Fig. 13, and exhibit a pronounced decrease at low temperatures consistent with decreasing population of low-lying excited states with S greater than that of the ground state. Extrapolation of the plot to 0 K, from temperatures above 6 K to avoid the effect of weak intermolecular interactions, gives a $\chi'_M T$ value of ~5.2 cm^3 K mol^{-1}, consistent with $S = 3$ and g < 2.0 ($\chi'_M T = 6$ cm^3 K mol^{-1} for $S = 3$ and $g = 2$) and thus in agreement with dc magnetization fit. Complex **4** did not exhibit an out-of-phase ac magnetic susceptibility signal down to 1.8 K (Fig. S2 in the ESI†), indicating that it is not a SMM; this is consistent with the low S and D values.

$Mn^{II}_2Mn^{III}_6$ clusters in the literature have $S = 4$ (or 5),[9c] 8,[9f] 1,[20a,60] 3,[36] 6[60] ground states. The $S = 3$ ground state of complex **4** has been previously encountered[36] in the cluster $[Mn^{II}_2Mn^{III}_6O_4(O_2CPh)_{12}(Et_2mal)_2(H_2O)_2]^-$ with a structure consisting of two linked butterfly units, and thus very different to that of **4**. An $S = 3$ state for a $Mn^{II}_2Mn^{III}_6$ cluster such as **4** that has spin values in the $S = 0$–17 range is consistent with a combination of both antiferro- (mainly) and ferromagnetic interactions, spin frustration effects within the fused triangular units in a completely antiferromagnetically coupled system, or both. There are various possible exchange interactions through mono- or diatomic bridging groups (Fig. 5), making it difficult to rationalize the observed spin value.

Conclusions

The present extension of the use of mpkoH ligand (and in general of 2-pyridyl oximate and pyridyl dioximate chelating/bridging ligands) in Mn cluster chemistry is a further demonstration of the ability of this group to yield products with interesting structures and magnetic properties. In addition to the $[Mn^{III}_3O(O_2CR')_3(mpko)_3]^+$ SMMs[19a–d] and the clusters $[Mn^{II}_4Mn^{III}_4O_2(OH)_2(O_2CR')_{10}(mpko)_4]$[19e] reported previously and prepared from Mn carboxylate sources, the Mn/X$^-$/mpkoH reaction systems have provided access to the ferromagnetically-coupled, trinuclear complex **3** (X$^-$ = Br$^-$) and the low-spin ($S = 3$), cationic octanuclear cluster **4** (X$^-$ = ClO_4^-). The former is a rare example of a non-triangular $Mn^{II}Mn^{IV}Mn^{II}$ complex, while the latter is a novel addition to the small subfamily

 This journal is © The Royal Society of Chemistry 2009

of octanuclear Mn clusters at the $Mn^{II}_2Mn^{III}_6$ level. Analogues of **3** and **4** with 2-pyridinecarbaldehyde oxime (paoH) or phenyl 2-pyridyl ketone oxime (ppkoH), see Scheme 1, are not known to date, and it is currently not evident whether the preparation and stability of such trinuclear and octanuclear complexes are dependent on the nature of the R substituent on the oxime carbon. Clearly, Mn/X^-/mpkoH non-carboxylate chemistry warrants further expansion to other X^- groups, *e.g.* N_3^-, NO_3^- and SO_4^{2-}. We are also pursuing our efforts to substitute the MeO^- bridge of **4** by an end-on bridging N_3^- group (η^1:μ), which is a known ferromagnetic coupler, to increase the ferromagnetic interactions within the molecule.

Acknowledgements

This work was supported by the Cyprus Research Promotion Foundation (Grant TEXNO/0506/06 to A.J.T.). The Advanced Light Source is supported by The Director, Office of Basic Energy Sciences, of the U.S. Department of Energy under Contract No. DE-AC02-05CH11231. S.P.P thanks the Operational and Vocational Training II (EPEAEK II) and particularly the program PYTHAGORAS (Grant b.365.037) for funding this research. G.C. thanks the National Science Foundation (CHE-0414555) for support of this work.

Notes and references

1 R. E. P. Winpenny, in *Comprehensive Coordination Chemistry II*, ed. J. A. McCleverty and T. J. Meyer, Elsevier, Amsterdam, 2004, vol. 7, pp. 125–175.
2 *Manganese Redox Enzymes*, ed. V. L. Pecoraro, VCH Publishers, New York, 1992.
3 (*a*) For a recent comprehensive review covering this topic, see: J. Barber and J. W. Murray, *Coord. Chem. Rev.*, 2008, **252**, 233; (*b*) K. N. Ferreira, T. M. Iverson, K. Maghlaoui, J. Barber and S. Iwata, *Science*, 2004, **303**, 1831.
4 (*a*) For a recent review, see: C. S. Mullins and V. L. Pecoraro, *Coord. Chem. Rev.*, 2008, **252**, 416; (*b*) I. J. Hewitt, J. K. Tang, N. T. Maddhu, R. Clérac, G. Buth, C. F. Anson and A. K. Powell, *Chem. Commun.*, 2006, 2650; (*c*) A. Mishra, W. Wernsdorfer, K. A. Abboud and G. Christou, *Chem. Commun*, 2005, 54.
5 (*a*) A. M. Ako, I. J. Hewitt, V. Mereacre, R. Clérac, W. Wernsdorfer, C. E. Anson and A. K. Powell, *Angew. Chem. Int. Ed.*, 2006, **45**, 4926; (*b*) Th. C. Stamatatos, K. A. Abboud, W. Wernsdorfer and G. Christou, *Angew. Chem. Int. Ed.*, 2007, **46**, 884; (*c*) M. Murugesu, M. Habrych, W. Wernsdorfer, K. A. Abboud and G. Christou, *J. Am. Chem. Soc.*, 2004, **126**, 4766; (*d*) Th. C. Stamatatos, K. A. Abboud, W. Wernsdorfer and G. Christou, *Angew. Chem. Int. Ed.*, 2006, **45**, 4134.
6 Th. C. Stamatatos and G. Christou, *Phil. Trans. R. Soc. A*, 2008, **366**, 113.
7 (*a*) For reviews, see: M. Murrie and D. J. Price, *Annu. Rep. Prog. Chem. Sect. A*, 2007, **103**, 20; (*b*) G. Aromi and E. K. Brechin, *Struct. Bonding*, 2006, **122**, 1; (*c*) R. Bircher, G. Chaboussant, C. Dobe, H. Güdel, S. T. Ochsenbein, A. Sieber and O. Waldman, *Adv. Funct. Mater.*, 2006, **16**, 209; (*d*) D. Gatteschi and R. Sessoli, *Angew. Chem. Int. Ed.*, 2003, **42**, 268; (*e*) J. R. Long, in *Chemistry of Nanostructured Materials*, ed. P. Yang, World Scientific Publishing, Hong Kong, 2003, p. 291; (*f*) G. Christou, D. Gatteschi, D. N. Hendrickson and R. Sessoli, *MRS Bull.*, 2000, **25**, 66.
8 G. Christou, *Polyhedron*, 2005, **24**, 2065, and references therein.
9 (*a*) M. Soler, W. Wernsdorfer, K. Folting, M. Pink and G. Christou, *J. Am. Chem. Soc.*, 2004, **126**, 2156; (*b*) C. Cañada-Vilalta, M. Pink and G. Christou, *Dalton Trans.*, 2003, 1121; (*c*) E. K. Brechin, G. Christou, M. Soler, M. Helliwell and S. J. Teat, *Dalton Trans.*, 2003, 513; (*d*) J. T. Brockman, Th. C. Stamatatos, W. Wernsdorfer, K. A. Abboud and G. Christou, *Inorg. Chem.*, 2007, **46**, 9160; (*e*) R. Bagai, K. A. Abboud and G. Christou, *Dalton Trans.*, 2006, 3306; (*f*) R. Bagai, K. A. Abboud and G. Christou, *Inorg. Chem.*, 2008, **47**, 621; (*g*) Th. C. Stamatatos, K. A. Abboud and G. Christou, *J. Mol. Struct.*, 2008, **890**, 263; (*h*) Th. C. Stamatatos, K. A. Abboud and G. Christou, *Dalton Trans.*, 2009, 41.
10 A. J. Tasiopoulos, A. Vinslava, W. Wernsdorfer, K. A. Abboud and G. Christou, *Angew. Chem. Int. Ed.*, 2004, **43**, 2117.
11 (*a*) Th. C. Stamatatos, K. A. Abboud, W. Wernsdorfer and G. Christou, *Polyhedron*, 2007, **26**, 2042; (*b*) Th. C. Stamatatos, K. M. Poole, K. A. Abboud, W. Wernsdorfer, T. A. O'Brien and G. Christou, *Inorg. Chem.*, 2008, **47**, 5006; (*c*) N. C. Harden, M. A. Bolcar, W. Wernsdorfer, K. A. Abboud, W. E. Streib and G. Christou, *Inorg. Chem.*, 2003, **42**, 7067; (*d*) C. Boskovic, E. K. Brechin, W. E. Streib, K. Folting, J. C. Bollinger, D. N. Hendrickson and G. Christou, *J. Am. Chem. Soc.*, 2002, **124**, 3725.
12 (*a*) E. K. Brechin, J. Yoo, J. C. Huffman, D. N. Hendrickson and G. Christou, *Chem. Commun.*, 1999, 783; (*b*) C. Boskovic, W. Wernsdorfer, K. Folting, J. C. Huffman, D. N. Hendrickson and G. Christou, *Inorg. Chem.*, 2002, **41**, 5107; (*c*) M. Murugesu, A. Mishra, W. Wernsdorfer, K. A. Abboud and G. Christou, *Polyhedron*, 2006, **25**, 613.
13 C. J. Milios, F. P. A. Fabbiani, S. Parsons, M. Murugesu, G. Christou and E. K. Brechin, *Dalton Trans.*, 2006, 351, and references therein.
14 (*a*) M. Murugesu, W. Wernsdorfer, K. A. Abboud and G. Christou, *Angew. Chem. Int. Ed.*, 2005, **44**, 892; (*b*) Th. C. Stamatatos, K. M. Poole, O. Foguet-Albiol, T. A. O'Brien and G. Christou, *Inorg. Chem.*, 2008, **47**, 6593.
15 D. Foguet-Albiol, T. A. O'Brien, W. Wernsdorfer, B. Moulton, M. J. Zaworotko, K. A. Abboud and G. Christou, *Angew. Chem. Int. Ed.*, 2005, **44**, 897.
16 (*a*) Th. C. Stamatatos, V. Nastopoulos, A. J. Tasiopoulos, E. E. Moushi, W. Wernsdorfer, G. Christou and S. P. Perlepes, *Inorg. Chem.*, 2008, **47**, 10081; (*b*) C. C. Stoumpos, I. A. Gass, C. J. Milios, N. Lalioti, A. Terzis, G. Aromi, S. J. Teat, E. K. Brechin and S. P. Perlepes, *Dalton Trans.*, 2009, 307; (*c*) Th. C. Stamatatos, K. A. Abboud, W. Wernsdorfer and G. Christou, *Angew. Chem., Int. Ed.*, 2008, **47**, 6694; (*d*) C. J. Milios, E. Kefalloniti, C. P. Raptopoulou, A. Terzis, R. Vicente, N. Lalioti, A. Escuer and S. P. Perlepes, *Chem. Commun.*, 2003, 819.
17 J. Yoo, E. K. Brechin, A. Yamaguchi, M. Nakano, J. C. Huffman, A. L. Maniero, L.-C. Brunel, K. Awaga, H. Ishimoto, G. Christou and D. N. Hendrickson, *Inorg. Chem.*, 2000, **39**, 3615.
18 (*a*) C. J. Milios, S. Piligkos and E. K. Brechin, *Dalton Trans.*, 2008, 1809; (*b*) C. J. Milios, A. Vinslava, P. A. Wood, S. Parsons, W. Wernsdorfer, G. Christou, S. P. Perlepes and E. K. Brechin, *J. Am. Chem. Soc.*, 2007, **129**, 8; (*c*) C. J. Milios, A. Vinslava, W. Wernsdorfer, S. Maggach, S. Parsons, S. P. Perlepes, G. Christou and E. K. Brechin, *J. Am. Chem. Soc.*, 2007, **129**, 2754; (*d*) C. J. Milios, A. Vinslava, W. Wernsdorfer, A. Prescimone, P. A. Wood, S. Parsons, S. P. Perlepes, G. Christou and E. K. Brechin, *J. Am. Chem. Soc.*, 2007, **129**, 6547; (*e*) C. J. Milios, R. Inglis, A. Vinslana, R. Bagai, W. Wernsdorfer, S. Parsons, S. P. Perlepes, G. Christou and E. K. Brechin, *J. Am. Chem. Soc.*, 2007, **129**, 12505; (*f*) C.-I. Yang, W. Wernsdorfer, G.-H. Lee and H.-L. Tsai, *J. Am. Chem. Soc.*, 2007, **129**, 456; (*g*) Th. C. Stamatatos, A. K. Boudalis, Y. Sanakis and C. P. Raptopoulou, *Inorg. Chem.*, 2006, **45**, 7372; (*h*) C. P. Raptopoulou, A. K. Boudalis, Y. Sanakis, V. Psycharis, J. M. Clemente-Juan, M. Fardis, G. Diamantopoulos and G. Papavassiliou, *Inorg. Chem.*, 2006, **45**, 2317; (*i*) T. Pathmalingam, S. I. Gorelsky, T. J. Burchell, A.-C. Béhard, A. M. Beauchemin, R. Clérac and M. Murugesu, *Chem. Commun.*, 2008, 2782.
19 (*a*) Th. C. Stamatatos, D. Foguet-Albiol, C. C. Stoumpos, C. P. Raptopoulou, A. Terzis, W. Wernsdorfer, S. P. Perlepes and G. Christou, *J. Am. Chem. Soc.*, 2005, **127**, 15380; (*b*) S.-C. Lee, Th. C. Stamatatos, D. Foguet-Albiol, S. Hill, S. P. Perlepes and G. Christou, *Polyhedron*, 2007, **26**, 2255; (*c*) Th. C. Stamatatos, D. Foguet-Albiol, S.-C. Lee, C. C. Stoumpos, C. P. Raptopoulou, A. Terzis, W. Wernsdorfer, S. O. Hill, S. P. Perlepes and G. Christou, *J. Am. Chem. Soc.*, 2007, **129**, 9484; (*d*) Th. C. Stamatatos, D. Foguet-Albiol, C. C. Stoumpos, C. P. Raptopoulou, A. Terzis, W. Wernsdorfer, S. P. Perlepes and G. Christou, *Polyhedron*, 2007, **26**, 2165; (*e*) C. C. Stoumpos, Th. C. Stamatatos, V. Psycharis, C. P. Raptopoulou, S. P. Perlepes and G. Christou, *Polyhedron*, 2008, **27**, 3703.
20 (*a*) Th. C. Stamatatos, B. S. Luisi, B. Moulton and G. Christou, *Inorg. Chem.*, 2008, **47**, 1134; (*b*) S. Khanra, T. Weyermüller and P. Chaudhuri, *Dalton Trans.*, 2008, 4885.
21 (*a*) For reviews, see: V. Yu. Kukushkin and A. J. L. Pombeiro, *Coord. Chem. Rev.*, 1999, **181**, 147; (*b*) A. G. Smith, P. A. Tasker and D. J. White, *Coord. Chem. Rev.*, 2003, **241**, 61; (*c*) P. Chaudhuri, *Coord. Chem. Rev.*, 2003, **243**, 143.

22 For a review, see: C. J. Milios, Th. C. Stamatatos and S. P. Perlepes, *Polyhedron*, 2006, **25**, 134 (Polyhedron Report).
23 (*a*) Selected work from our group: M. Murugesu, K. A. Abboud and G. Christou, *Polyhedron*, 2004, **23**, 2779; (*b*) Th. C. Stamatatos, K. A. Abboud, S. P. Perlepes and G. Christou, *Dalton Trans.*, 2007, 3861; (*c*) C. Papatriantafyllopoulou, G. Aromi, A. J. Tasiopoulos, V. Nastopoulos, C. P. Raptopoulou, S. J. Teat, A. Escuer and S. P. Perlepes, *Eur. J. Inorg. Chem.*, 2007, 2761; (*d*) Th. C. Stamatatos, E. Diamantopoulou, C. P. Raptopoulou, V. Psycharis, A. Escuer and S. P. Perlepes, *Inorg. Chem.*, 2007, **46**, 2350; (*e*) Th. C. Stamatatos, E. Diamantopoulou, A. Tasiopoulos, V. Psycharis, R. Vicente, C. P. Raptopoulou, V. Nastopoulos, A. Escuer and S. P. Perlepes, *Inorg. Chim. Acta*, 2006, **359**, 4149.
24 (*a*) R. Clérac, H. Miyasaka, M. Yamashita and C. Coulon, *J. Am. Chem. Soc.*, 2002, **124**, 12837; (*b*) H. Miyasaka, R. Clérac, K. Mizushima, K. Sugiura, M. Yamashita, W. Wernsdorfer and C. Coulon, *Inorg. Chem.*, 2003, **42**, 8203.
25 M. Orama, H. Saarinen and J. Korvenranta, *J. Coord. Chem.*, 1990, **22**, 183.
26 G. M. Sheldrick, *SHELXS-97, Program for Crystal Structure Solution*, University of Göttingen, Germany, 1997.
27 G. M. Sheldrick, *SHELXL-97, Program for the Refinement of Crystal Structures from Diffraction Data*, University of Göttingen, Germany, 1997.
28 *CrysAlis CCD and CrysAlis RED, Version 1.171.32.15*, Oxford Diffraction Ltd., Abingdon, Oxford, England, 2008.
29 *SIR 2002*, M. C. Burla, M. Camalli, B. Carrozzini, G. L. Cascarano, C. Giacovazzo, G. Polidori and R. Spagna, *J. Appl. Crystallogr.*, 2003, **36**, 1103.
30 *WINGX*, L. J. Farrugia, *J. Appl. Crystallogr.*, 1999, **32**, 837.
31 A. L. Spek, *PLATON-A Multipurpose Crystallographic Tool*, University of Utrecht, the Netherlands, 2008.
32 *MERCURY*, C. F. Macrae, P. R. Edgington, P. McCabe, E. Pidcock, G. P. Shields, R. Taylor, M. Towler and J. van de Streek, *J. Appl. Crystallogr*, 2006, **39**, 453.
33 K. Brandenburg, *DIAMOND, Release 3.1f, Crystal Impact GbR*, Bonn, Germany, 2008.
34 (*a*) H.-L. Tsai, S. Wang, K. Folting, W. E. Streib, D. N. Hendrickson and G. Christou, *J. Am. Chem. Soc.*, 1995, **117**, 2503; (*b*) R. C. Squire, S. M. J. Aubin, K. Folting, W. E. Streib, G. Christou and D. N. Hendrickson, *Inorg. Chem.*, 1995, **34**, 6463.
35 J. B. Vincent, H.-R. Chang, K. Folting, J. C. Huffman, G. Christou and D. N. Hendrickson, *J. Am. Chem. Soc.*, 1987, **109**, 5703.
36 M. W. Wemple, H.-L. Tsai, S. Wang, J. P. Claude, W. E. Streib, J. C. Huffman, D. N. Hendrickson and G. Christou, *Inorg. Chem.*, 1996, **35**, 6437.
37 N. E. Chakov, W. Wernsdorfer, K. A. Abboud and G. Christou, *Inorg. Chem.*, 2004, **43**, 5919.
38 (*a*) A. N. Singh and A. Chakravorty, *Inorg. Chem.*, 1980, **19**, 969; (*b*) H.-J. Krüger, G. Peng and R. H. Holm, *Inorg. Chem.*, 1991, **30**, 734.
39 (*a*) C. J. Milios, Th. C. Stamatatos, P. Kyritsis, A. Terzis, C. P. Raptopoulou, R. Vicente, A. Escuer and S. P. Perlepes, *Eur. J. Inorg. Chem.*, 2004, 2885; (*b*) K. W. Nordquest, D. W. Phelps, W. F. Little and D. J. Hodgson, *J. Am. Chem. Soc.*, 1976, **98**, 1104.
40 A. B. P. Lever and E. Mantovani, *Inorg. Chem.*, 1971, **10**, 817.
41 (*a*) P. Chaudhuri, M. Winter, U. Flörke and H.-J. Houpt, *Inorg. Chim. Acta*, 1995, **232**, 125; (*b*) C. Papatriantafyllopoulou, C. P. Raptopoulou, A. Terzis, E. Manessi-Zoupa and S. P. Perlepes, *Z. Naturforsch*, 2006, **61b**, 37.
42 R. D. Cannon and R. P. White, *Prog. Inorg. Chem.*, 1988, **36**, 195.
43 K. Nakamoto, *Infrared and Raman Spectra of Inorganic and Coordination Compounds*, Wiley, New York, 4th edn, 1986, pp. 139, 251.
44 (*a*) I. D. Brown and D. Altermatt, *Acta Crystallogr.*, 1985, **B41**, 244; (*b*) W. Liu and H. H. Thorp, *Inorg. Chem.*, 1993, **32**, 4102.
45 R. van Gorkum, F. Buda, H. Kooijman, A. L. Spek, E. Bouwman and J. Reedijk, *Eur. J. Inorg. Chem.*, 2005, 2255.
46 K. F. Purcell and J. C. Kotz, *Inorganic Chemistry*, Saunders, Philadelphia, USA, 1977, pp. 587–590, 600–603.
47 For a review, see: D. P. Kessissoglou, *Coord. Chem. Rev.*, 1999, **185–186**, 837.
48 (*a*) For example, see: R. T. W. Scott, S. Parsons, M. Murugesu, W. Wernsdorfer, G. Christou and E. K. Brechin, *Chem. Commun.*, 2005, 2083; (*b*) S. Yano, M. Doi, S. Tamakoshi, W. Mori, M. Mikuriya, A. Ichimura, I. Kinoshita, Y. Yamamoto and T. Tanase, *Chem. Commun.*, 1997, 997; (*c*) X. S. Tan, J. Sun, C. H. Hu, D. G. Fu, D. F. Xiang, P. J. Zheng and W. X. Tang, *Inorg. Chim. Acta*, 1997, **257**, 203.
49 (*a*) For example, see: M. Hirotsu, M. Kojima, W. Mori and Y. Yoshikawa, *Bull. Chem Soc. Jpn.*, 1998, **71**, 2873; (*b*) V. Pavlishchuk, F. Birkelbach, T. Weyhermüller, K. Wieghardt and P. Chaudhuri, *Inorg. Chem.*, 2002, **41**, 4405; (*c*) Y.-G. Li, L. Lecren, W. Wernsdorfer and R. Clérac, *Inorg. Chem. Commun*, 2004, **7**, 1281; (*d*) V. Tangoulis, D. A. Malamatari, K. Soulti, V. Stergiou, C. P. Raptopoulou, A. Terzis, T. A. Kabanos and D. P. Kessissoglou, *Inorg. Chem.*, 1996, **35**, 4974.
50 A. A. Danopoulos, G. Wilkinson, T. K. N. Sweet and M. B. Hursthouse, *J. Chem. Soc., Dalton Trans.*, 1995, 937.
51 (*a*) M. Alexiou, C. Dendrinou-Samara, A. Karagianni, S. Biswas, C. M. Zaleski, J. Kampf, D. Yoder, J. E. Penner-Hahn, V. L. Pecoraro and D. P. Kessissoglou, *Inorg. Chem.*, 2003, **42**, 2185; (*b*) M. Alexiou, C. M. Zaleski, C. Dendrinou-Samara, J. Kampf, D. P. Kessissoglou and V. L. Pecoraro, *Z. Anorg. Allg. Chem.*, 2003, **629**, 2348.
52 C. Mukherjee, Th. Weyhermüller, K. Wieghardt and P. Chaudhuri, *Dalton Trans.*, 2006, 2169.
53 (*a*) G. Karotsis, L. F. Jones, G. S. Papaefstathiou, A. Collins, S. Parsons, T. D. Nguyen, M. Evangelisti and E. K. Brechin, *Dalton Trans.*, 2008, 4917; (*b*) C. J. Milios, S. Piligkos, A. R. Bell, R. H. Laye, S. J. Teat, R. Vicente, E. McInnes, A. Escuer, S. P. Perlepes and R. E. P. Winpenny, *Inorg. Chem. Commun.*, 2006, **9**, 638; (*c*) T. Afrati, C. Dendrinou-Samara, C. P. Raptopoulou, A. Terzis, V. Tangoulis and D. P. Kessissoglou, *Angew. Chem. Int. Ed.*, 2002, **41**, 2148.
54 A. W. Addison, T. N. Rao, J. Reedijk, J. Rijn and G. C. Verschoor, *J. Chem. Soc., Dalton Trans.*, 1984, 1349.
55 N. E. Chakov, S.-C. Lee, A. G. Harter, P. L. Kuhns, A. P. Reyes, S. O. Hill, N. S. Dalal, W. Wernsdorfer, K. A. Abboud and G. Christou, *J. Am. Chem. Soc.*, 2006, **128**, 6975.
56 A. Mishra, A. J. Tasiopoulos, W. Wernsdorfer, K. A. Abboud and G. Christou, *Inorg. Chem.*, 2007, **46**, 3105.
57 (*a*) P. Crewdson, S. Gambarotta, C. P. A. Yap and L. K. Thompson, *Inorg. Chem.*, 2003, **42**, 8579; (*b*) C. S. Alvarez, A. D. Bond, D. Cave, M. E. G. Mosquera, E. A. Harron, R. A. Layfield, M. McPartlin, J. W. Rawson, P. T. Wood and D. S. Wright, *Chem. Commun.*, 2002, 2980; (*c*) R. W. Saalfrank, N. Löw, B. Demleitner, D. Stalke and M. Teichert, *Chem.–Eur. J.*, 1998, **4**, 1305; (*d*) R. W. Saalfrank, N. Löw, S. Trummer, G. M. Sheldrick, M. Teichert and D. Stalke, *Eur. J. Inorg. Chem.*, 1998, 559; (*e*) L. B. Jerzykiewicz, J. Utko, M. Duczmal and P. Sobota, *Dalton Trans.*, 2007, 825.
58 C. Boskovic, J. C. Huffman and G. Christou, *Chem. Commun.*, 2002, 2502.
59 M. Manoli, C. J. Milios, A. Mishra, G. Christou and E. K. Brechin, *Polyhedron*, 1923, **26**.
60 C. J. Milios, R. Inglis, A. Vinslava, A. Prescimone, S. Parsons, S. P. Perlepes, G. Christou and E. K. Brechin, *Chem. Commun.*, 2007, 2738.
61 (*a*) M. D. Godbole, O. Roubeau, R. Clérac, H. Kooijman, A. L. Spek and E. Bouwman, *Chem. Commun.*, 2005, 3715; (*b*) E. K. Brechin, M. Soler, G. Christou, M. Helliwell, S. J. Teat and W. Wernsdorfer, *Chem. Commun.*, 2003, 1276; (*c*) G. Rajaraman, M. Murugesu, E. C. Sanudo, M. Soler, W. Wernsdorfer, M. Helliwell, C. Muryn, J. Raftery, S. J. Teat, G. Christou and E. K. Brechin, *J. Am. Chem. Soc.*, 2004, **126**, 15445; (*d*) L. F. Jones, E. K. Brechin, D. Collison, J. Raftery and S. J. Teat, *Inorg. Chem.*, 2003, **42**, 6971; (*e*) S. Wang, J. C. Huffman, K. Folting, W. E. Streib, E. B. Lobkovsky and G. Christou, *Angew. Chem. Int. Ed.*, 1991, **30**, 1672; (*f*) S. Tanase, G. Aromi, E. Bouwman, H. Kooijman, A. L. Spek and J. Reedijk, *Chem. Commun.*, 2005, 3147; (*g*) S. Wang, H.-L. Tsai, K. Folting, J. D. Martin, D. N. Hendrickson and G. Christou, *Chem. Commun.*, 1994, 671; (*h*) R. P. John, K. Lee, B. J. Kim, B. J. Suh, H. Rhee and M. S. Lah, *Inorg. Chem.*, 2005, **44**, 7109; (*i*) V. A. Grillo, M. J. Knapp, J. C. Bollinger, D. N. Hendrickson and G. Christou, *Angew. Chem. Int. Ed.*, 1996, **35**, 1818; (*j*) E. Libby, K. Folting, J. C. Huffman and G. Christou, *J. Am. Chem. Soc.*, 1990, **112**, 5354.
62 A. J. Tasiopoulos, K. A. Abboud and G. Christou, *Chem. Commun.*, 2003, 580.
63 (*a*) O. Roubearu, L. Lecren, Y.-G. Li, X. L. Le Goff and R. Clérac, *Inorg. Chem. Commun.*, 2005, **8**, 314; (*b*) C. Dendrinou-Samara, C. M. Zaleski, A. Evagorou, J. W. Kampf, V. L. Pecoraro and D. P. Kessissoglou, *Chem. Commun.*, 2003, 2668; (*c*) C. M. Zaleski, T.-C. Weng, C. Dendrinou-Samara, M. Alexiou, P. Kanakaraki, W.-Y. Hsieh, J. Kampf, J. E.

 This journal is © The Royal Society of Chemistry 2009

Penner-Hahn, V. L. Pecoraro and D. P. Kessissoglou, *Inorg. Chem.*, 2008, **47**, 6127; (*d*) C. J. Milios, P. Kyritsis, C. P. Raptopoulou, A. Terzis, R. Vicente, A. Escuer and S. P. Perlepes, *Dalton Trans.*, 2005, 501.
64 J. K. Kambe, *J. Phys. Soc. Jpn.*, 1950, **5**, 48.
65 E. R. Davidson, *MAGNET*, Indiana University, Bloomington, IN, 1999.
66 E. R. Davidson, *GRID*, Indiana University, Bloomington, IN, 1999.
67 For example, see: T. Taguchi, Th. C. Stamatatos, K. A. Abboud, C. M. Jones, K. M. Poole, T. A. O'Brien and G. Christou, *Inorg. Chem.*, 2008, **47**, 4094.
68 (*a*) P. King, W. Wernsdorfer, K. A. Abboud and G. Christou, *Inorg. Chem.*, 2005, **44**, 8659; (*b*) A. J. Tasiopoulos, W. Wernsdorfer, K. A. Abboud and G. Christou, *Inorg. Chem.*, 2005, **44**, 6324.